1990A&A...240..142M

Astron. Astrophys. 240, 142–149 (1990)

ASTRONOMY AND ASTROPHYSICS

Buoyancy-limited thin shell dynamos

D. Moss*, I. Tuominen, and A. Brandenburg

Observatory and Astrophysics Laboratory, University of Helsinki, Tähtitorninmäki, SF-00130 Helsinki, Finland

Received March 13, accepted May 16, 1990

Abstract. We have investigated axisymmetric nonlinear mean-field dynamos in spherical shells that attempt to model the gross effects of a dynamo operating in a thin layer at the base of a convective envelope. A form of magnetic buoyancy restricts the fields to finite amplitude. As the shell thickness decreases the excitation conditions and spatial structure of even and odd parity modes become almost identical. For very thin shells the field forms a number of almost disjoint cells. We also found mixed parity solutions which typically evolved very slowly towards pure odd or even parity solutions. The time scale of these slow variations is of the order of a hundred global diffusion times. We were unable to find completely steady (averaged over a cycle) mixed parity solutions.

Key words: dynamos: nonlinear – buoyancy – magnetohydrodynamics – solar cycle

1. Introduction

Considerable interest has been expressed in the last decade or so in the idea that the solar cycle is driven by a dynamo situated near the bottom of the solar convection zone. Inter alia, this model has been proposed as a way of avoiding excessive flux loss by magnetic buoyancy that might, for example, quench the dynamo at an unacceptably small amplitude. The buoyancy of flux tubes may be an essential ingredient of the nonlinear limitation of the solar dynamo (cf. Noyes et al. 1984). The effect of such flux removal on the solar dynamo has commonly been investigated with one-dimensional models in which the radial extent of the convection zone is omitted (e.g. Leighton 1969; Schmitt & Schüssler 1989; Jennings & Weiss 1990). However the consequences of such a drastic simplification are unclear, and the approximation is very questionable.

In a previous paper we investigated the influence of a simple parameterization of magnetic buoyancy on solutions of the axisymmetric dynamo equations in full two-dimensional geometry (Moss et al. 1990, henceforth Paper I). This paper studied a mean-field dynamo with sources (α-effect, differential rotation) distributed uniformly throughout a spherical volume. The axisymmetric dynamo equations were solved in full two-dimensional geometry. In contrast to one-dimensional models of nonlinear buoyancy-limited dynamos (e.g. Jennings & Weiss 1990) and also to two-dimensional α-quenched models (Brandenburg et al. 1989), the buoyancy-limited solutions of Paper I did not exhibit any long term behaviour that was more complex than a simple limit cycle. It was speculated that this could possibly be because of the uniform source distribution, or perhaps because of the comparatively restricted range of parameters that were accessible to the code used.

Bearing all these factors in mind, here we develop a two-dimensional model for a "thin shell", buoyancy limited $\alpha^2\omega$ dynamo that might be situated near the base of a stellar convection zone.

Send offprint requests to: D. Moss (permanent address)

*Permanent address: Mathematics Department, The University, Manchester M13 9PL, UK

2. The model

We are interested in solving the mean field dynamo equation in a spherical shell $R_1 \le r \le R_2$. We adopt a mean field formulation of the dynamo problem, with isotropic α effect.

2.1. Buoyancy

The representation in the mean field dynamo equation of the effect of magnetic buoyancy in removing flux is to some extent arbitrary, in that different authors adopt different representations. In the literature a modification of the induction equation of the form

$$\frac{\partial \boldsymbol{B}}{\partial t} = \ldots\ldots - \frac{\boldsymbol{B}}{\tau} f(|B|) \tag{1}$$

has often been discussed (e.g. DeLuca & Gilman 1986). Such a form was first considered by Leighton (1969) and more recently by Schmitt & Schüssler (1989) and Jennings & Weiss (1990). Referring to the early work of Leighton (1969), DeLuca & Gilman (1986) applied Eq. (1) also to the case where the radial extent is retained. However, Rädler (1990) has stressed that this is hardly the correct way to comprehend the action of magnetic buoyancy, and that the overall effect should be merely to modify the electromotive force, i.e. to provide an extra term under the curl operator, cf. Eq. (5) (below).

As in Paper I we represent the effect of magnetic buoyancy by introducing a macroscopic velocity.

$$\boldsymbol{u}_B = f(\boldsymbol{B})\hat{\boldsymbol{r}}, \tag{2}$$

into the dynamo equation. $\boldsymbol{u}_B$ might be considered to be related to the radial velocity of buoyant flux tubes (see Paper I; see also

© European Southern Observatory • Provided by the NASA Astrophysics Data System

1990A&A...240..142M

Krivodubskii 1984). We use

$$f(\boldsymbol{B}) = \Gamma|\boldsymbol{B}| \tag{3}$$

in the calculations described below, although results outlined in Paper I suggest that the choice is not crucial to the qualitative nature of the results and that, e.g., $f(\boldsymbol{B}) \propto \boldsymbol{B}^2$ would give similar behaviour. Γ is assumed to be constant in the outer 80% of the computational shell, but is made to tend smoothly to zero at the inner boundary.

The velocity $\boldsymbol{u}_B$ defined by Eqs. (2) and (3) appears to violate mass continuity. However $\boldsymbol{u}_B$ is a mean-field velocity, derived from a buoyant velocity that supposedly acts predominantly in regions of high field strength, where it is always in the outward direction. The return flow is considered to be diffuse, of smaller magnitude, in regions of substantially lower field strength. Thus the mean velocity experienced by $\boldsymbol{B}$ can be taken to be of the form (3) with $\Gamma > 0$, without implying any overall violation of the mass continuity constraint.

2.2. *The model equations*

We only consider axisymmetric magnetic fields and so can split $\boldsymbol{B}$ into poloidal and toroidal parts and write

$$\boldsymbol{B} = \nabla \times (a\hat{\boldsymbol{\varphi}}) + b\hat{\boldsymbol{\varphi}}, \tag{4}$$

referred to a spherical polar coordinate system (r, θ, φ). The mean field dynamo equation in dimensionless form can be written as

$$\partial \boldsymbol{B}/\partial t = \nabla \times (C_\omega \boldsymbol{u} \times \boldsymbol{B} + \gamma|\boldsymbol{B}|\hat{\boldsymbol{r}} \times \boldsymbol{B} + C_\alpha \cos\theta \boldsymbol{B}) - \nabla \times \nabla \times \boldsymbol{B}, \tag{5}$$

where we have scaled time in units of R_2^2/η, where η is the resistivity, assumed to be uniform and $\boldsymbol{B}$ is now a dimensionless field, measured in units of $\boldsymbol{B}^*$, say. $\boldsymbol{u}$ is a prescribed differential rotation, i.e. $\boldsymbol{u} = \Omega x \sin\theta \hat{\boldsymbol{\varphi}}$, $x = r/R_2$ and we take $\alpha = \tilde{\alpha}(x)\cos\theta$.

As usual we solve the φ component of Eq. (5) and the φ component of the equation obtained by "uncurling" Eq. (5), for b and a respectively. The dynamo parameters are given by

$$C_\alpha = \alpha_0 R_2/\eta, \quad C_\omega = \Omega_0' R_2^3/\eta,$$

$$\gamma = \Gamma B^* \frac{R_2}{\eta}, \quad \text{and} \quad \Omega = \frac{2x - x_1 - x_2}{2(x_2 - x_1)}\Omega_0', \tag{6}$$

where $x_2 = 1$ by definition and Ω_0' is assumed to be constant. As discussed in Paper I the equations can be scaled to remove γ as a free parameter and so we take the value of γ throughout the bulk of the shell to be unity.

2.3. *Boundary conditions and α-profile*

The two equations derived from (5) were solved in the shell $R_1 \le r \le R_2$ (i.e. $x_1 \le x \le 1$), $0 \le \theta \le \pi$ by the method described in Paper I. The computational grid contained NI points uniformly distributed in x and NJ points uniformly distributed in θ. Note that we do not impose any boundary conditions that preselect solutions of a particular parity with respect to the equatorial plane and that solutions of mixed parity are thus permitted.

We considered two distinct boundary conditions at $r = R_1$. The first is a simple minded approximation to the physical condition that an oscillating dynamo field will be almost completely excluded from the underlying, relatively highly conducting, radiative region by the skin effect. (Our main concern in a solar context is, of course with oscillating fields.) In this case we take $B_r = B_\varphi = 0$ at $r = R_1$, i.e.

$$a = b = 0 \quad \text{where} \quad x = x_1, \tag{7}$$

recognizing that this means that B_θ will in general be non-zero there (and so there must be a surface current J_φ on $r = R_1$). The other form of boundary condition explicitly assumes the region $r < R_1$ to be a perfect electrical conductor, in which case the boundary conditions are

$$a = 0, \ \alpha\partial(ar)/\partial r = \eta\partial(br)/\partial r \quad \text{on} \quad r = R_1. \tag{8}$$

(With η constant in $r > R_1$ this implies $B_\varphi \neq 0$ at $r = R_1$ and so there is now a surface current J_θ on $r = R_1$. The perfect conductor condition

$$\alpha B_\varphi = \eta(\nabla \times \boldsymbol{B})_\varphi$$

is satisfied identically at $r = R_1$ by the dynamo equation for a, given the first of conditions (8).) We only used the boundary conditions (7) for the "thick shell" calculation with $x_1 = 0.7$ (Sect. 3.1). In this case we verified that our results and those obtained using the perfect conductor condition (8) were very similar: the poloidal field lines were almost identical and the toroidal field contours differed only towards the base of the shell. The oscillation periods were very similar and the only significant difference was a change in the mean energies, typically by about 20%. Initially we formulated a model that might be considered to represent the complete convective envelope of a late type star, with

$$\alpha = \frac{\alpha_0 \cos\theta \, 15(\zeta^2 - 1)^2}{16(x_u - x_2)}, \quad x \le x_u, \quad \alpha = 0, \quad x > x_u.$$

where

$$\zeta = \frac{(x - x_1)}{x_u - x_1}$$

and $x_u (> x_1)$ is a radius beyond which the α effect is assumed not to operate. In this case $r = R_2$ (i.e. $x = x_2 = 1$) corresponds to the stellar surface and so we adopted the usual boundary conditions, that the toroidal field be zero at $x = 1$ and that the poloidal field fit smoothly on to a curl-free exterior field there.

Taking $x_1 = 0.7$, $x_u = 0.8$, we were able to compute some oscillatory dynamos with this model, but only for a very limited range of C_ω, even with a resolution of NI = 41, NJ = 81. A quite small increase in C_ω or C_α necessitated a finer computational mesh for numerical accuracy and, what was worse, the scheme displayed signs of numerical instability. We therefore abandoned our study of this model. We did, however, note that typically the the poloidal field lines ($ax \sin\theta$ = constant) and contours of toroidal field (b = constant) were approximately radial over a large extent in θ in the region where α became small.

These experiences led us to try to develop a simpler model of the region of dynamo excitation only, without calculating explicitly the field evolution and structure in the overlaying outer envelope region (considered to be passive, apart perhaps from the effects of differential rotation). Thus our shell $R_1 \le r \le R_2$ now is to be thought of as representing a region near the base of a convective envelope. The boundary conditions at $r = R_2$ are no longer that the field fits onto a curl-free exterior field but, guided

© European Southern Observatory • Provided by the NASA Astrophysics Data System

1990A&A...240..142M

to some extent by our previous results, we apply the conditions

$$\partial a/\partial x = \partial b/\partial x = 0 \quad \text{at} \quad x = x_2 = 1, \tag{9}$$

and we now take $\tilde{\alpha}(x)$ = constant throughout the shell volume. The poloidal field would be strictly radial if $\partial(ax)/\partial x = 0$, but in practice the first of conditions (9) gives a poloidal field that is quite close to being radial. This corresponds physically to a situation in which poloidal field lines are being 'lifted' up into the overlying region, and in which the toroidal field is continuous with that of the overlying region into which it rises. Note that we continue to scale lengths with the outer radius of the shell, R_2, and so our calculations still cover the region $x_1 \leq x \leq 1$, and it must be remembered that $x = 1$ is deep inside the envelope region and does not correspond to the 'surface'. For example, if the centre of our shell were thought to be at about 70% of the stellar radius then the fractional radial extent of the shell would be approximately $0.7(1-x_1)$. We shall present results for a "thick shell" with $x_1 = 0.7$ and a "thin shell" with $x_1 = 0.9$. Typically our computational grid had NI = 41, NJ = 81 and the timestep was 5 or 2.5×10^{-5}. Some results were confirmed with NI = 81, NJ = 161.

3. Numerical results

3.1. Thick shell $x_1 = 0.7$

Using the boundary conditions (7) corresponding to the field being completely excluded from $x < x_1$, we first computed α^2

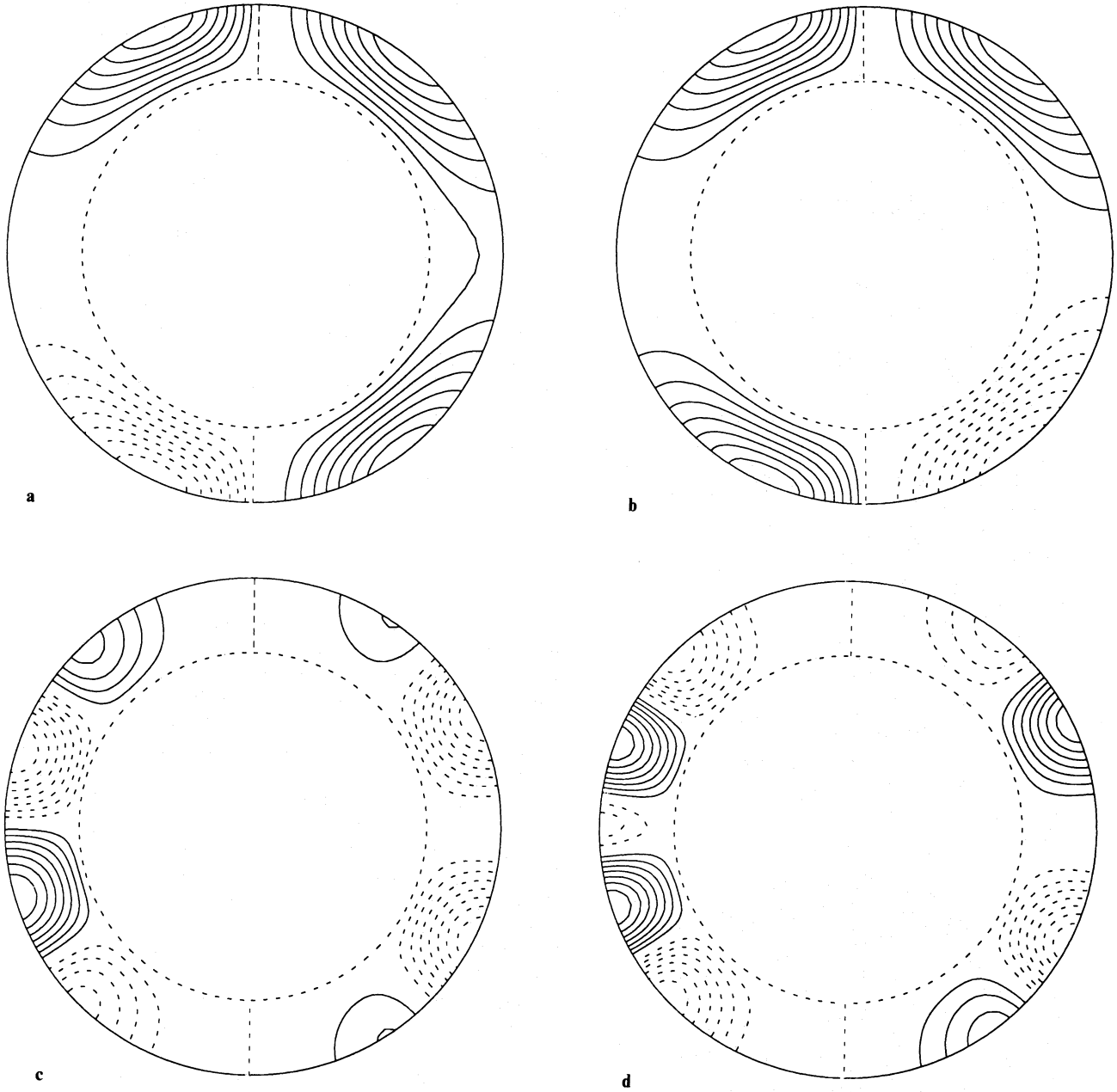

Fig. 1a–d. $x_1 = 0.7$. Field structures of eigenmodes, **a** $C_\omega = 0$, A0 mode, **b** $C_\omega = 0$, S0 mode, **c** $C_\omega = -10^3$, A0 mode, **d** $C_\omega = -10^3$, S0 mode. The left half of each figure shows contours of equal toroidal field strength, right half shows poloidal field lines. Dashed contours represent negative values of *b* or *a* respectively. Note that when $C_\omega = -10^3$ the field is oscillatory, and the fields illustrated in **c** and **d** are not at exactly corresponding phases

© European Southern Observatory • Provided by the NASA Astrophysics Data System

1990A&A...240..142M

modes (i.e. $C_\omega = 0$) taking a clearly supercritical value, $C_\alpha = 10$. These solutions are steady. Field lines for the odd and even (A0 and S0) modes are shown in Fig. 1a and b. We then investigated $\alpha^2\omega$ solutions with C_ω held constant at -10^3. These solutions are oscillatory, and the bifurcations from the trivial solution occur at $C_\alpha \approx 1.25$. The values for the odd and even modes were very similar and we did not separate them. Eigenmodes are shown in Fig. 1c and d. Following our previous work (Brandenburg et al. 1989; Paper I), we defined the parity parameter

$$P = (E^{(S)} - E^{(A)})/(E^{(S)} + E^{(A)}),$$

where $E^{(S)}$ and $E^{(A)}$ are the energies in the parts of the field respectively symmetric (even) and antisymmetric (odd) with respect to the rotational equator. Thus an A0 mode has $P = -1$ and a S0 mode has $P = +1$. We constructed initial fields of mixed parity, $-1 < P(0) < 1$. Taking $C_\alpha = 3$, we evolved these until the solutions exhibited a quite steady cyclic behaviour. In each case by $t \approx 0.5$ the total magnetic energy E settled to a steady oscillation with mean value, amplitude and period independent of $P(0)$, but at this time (in contrast to the α^2 models) the corresponding parity parameters $P(t)$ depended markedly on $P(0)$ (see Fig. 2). In each case $\langle P \rangle$, the mean value of P over a cycle, appeared at first sight to be almost constant, but a closer examination of the results in each case showed that P was performing a limit cycle of small amplitude. Moreover this amplitude appeared to be slowly changing, in the direction of $P = -1$, although the rate of change is very small (and at $t \leq 1$, at least, depends somewhat on $P(0)$ with $\mathrm{d}\langle P \rangle/\mathrm{d}t \approx -0.03$ when P is near 0.9 and -0.01 when P is near -0.9, for example), and so the long term behaviour of these solutions is uncertain, especially in the light of some rather similar behaviour studied in detail in Paper I (see, e.g. Sect. 4.2.3 of that paper). The timescale for these long term variations is typically 30–100 diffusion times (in units of R_2^2/η).

We performed a similar exercise at $C_\alpha = 10$ (see Fig. 3), with broadly similar results, except that now any trend of $\langle P \rangle$ with time after the initial relaxation was much less obvious. Although P appears to be varying quite uniformly, a closer inspection reveals some structure in the pulse shape (see the inset in Fig. 3).

Finally we made a sequence of calculations, starting with $P(0) = 0$, but with C_α varying in the range 1.5 to 10. We give in Table 1 the magnitude and amplitude of the oscillation in log E and the behaviour of P after the initial relaxation phase. The period decreases as C_α increases. This is in agreement with previous results (Paper I). Figure 4 shows typical field configurations for mixed mode solutions for $C_\alpha = 3$ and $C_\alpha = 10$. When $C_\alpha = 20$ the structure is similar, except that there is then an additional 'cell' in the θ-extent.

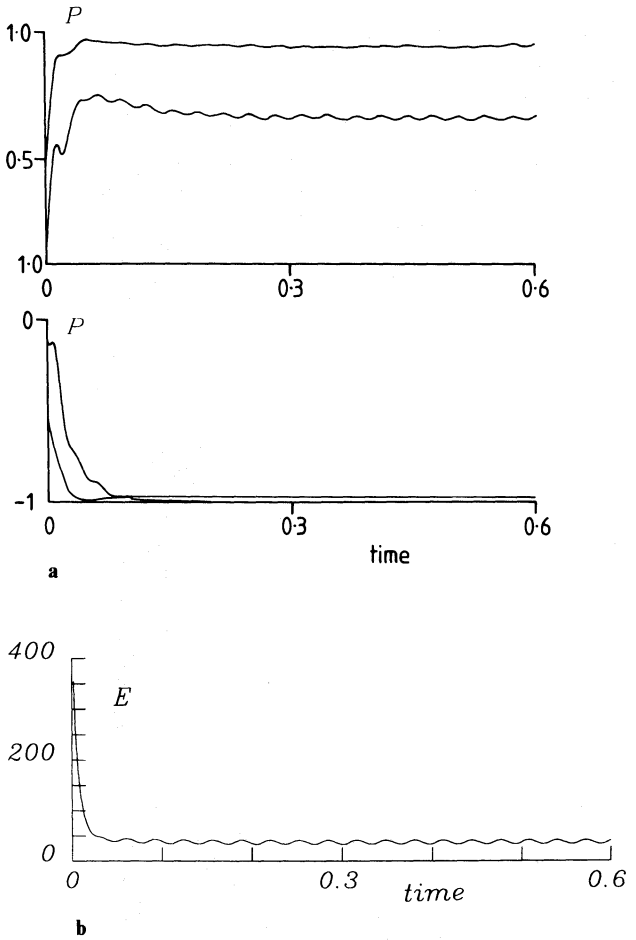

Fig. 2a and b. $x_1 = 0.7$. **a** Evolution of $P(t)$ for $C_\omega = -10^3$, $C_\alpha = 3$ for selected $P(0)$. **b** Evolution of E for $P(0) = 0.1$

3.2. *Thin shell* $x_1 = 0.9$

In this case we adopted the perfect conductor conditions (8) at the lower boundary, in contrast to those used in Sect. 3.1. Experiments suggest that although, for example, the energy at saturation and the position of the bifurcations do depend somewhat on the choice of boundary conditions, the overall nature of the results is little affected. We only investigated $\alpha^2\omega$ models with

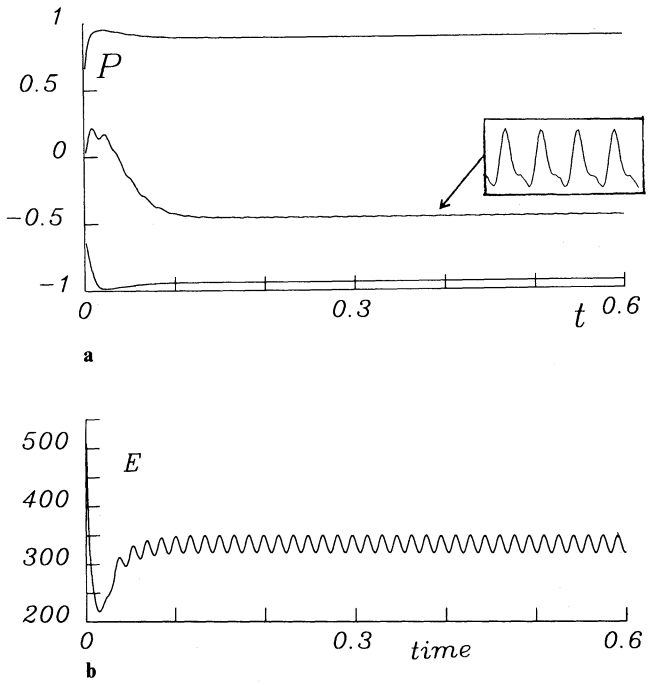

Fig. 3a and b. $x_1 = 0.7$. **a** Evolution of $P(t)$ for $C_\omega = -10^3$, $C_\alpha = 10$. $P(0)$ varies. The inset shows pulse structure of $P(t)$ for the case $P(0) = 0$. **b** Evolution of E for $P(0) = 0.0$

© European Southern Observatory • Provided by the NASA Astrophysics Data System

1990A&A...240..142M

$C_\omega = -10^3$. A0 and S0 modes were both excited at $C_\alpha \approx 2.8$, and the eigenmodes are shown in Fig. 5.

Following the pattern described in Sect. 3.1 we followed the field evolution from a standard set of initial fields of intermediate parity for both $C_\alpha = 10$ and $C_\alpha = 4$. By $t = 0.25$ the mean behaviour had become steady, with the energy saturating at an amplitude and period independent of the initial conditions to within the accuracy of the computations. (Although the variation of the total energy during a cycle is relatively small, this is because of the quite complex spatial structure of the field, and the field values at any given points vary very much more markedly.) However the overall behaviour of the parity parameter P was in each case more complex (see Fig. 6). We could not really be sure that the limit cycles exhibited by P were steady, but if they were evolving steadily with time then $|\mathrm{d}\langle P\rangle/\mathrm{d}t|$ is smaller than for the thick shell (Sect. 3.1). Thus it appears that the long-term variation of the mean parity parameter occurs more slowly when the shell thickness is smaller.

Finally we followed the field evolution from an initial state with $P(0) = 0$ for different values of C_α. These results are shown in Fig. 7 and summarized in Table 2. Typical field configurations with $C_\alpha = 3$ and $C_\alpha = 10$ are shown in Fig. 8.

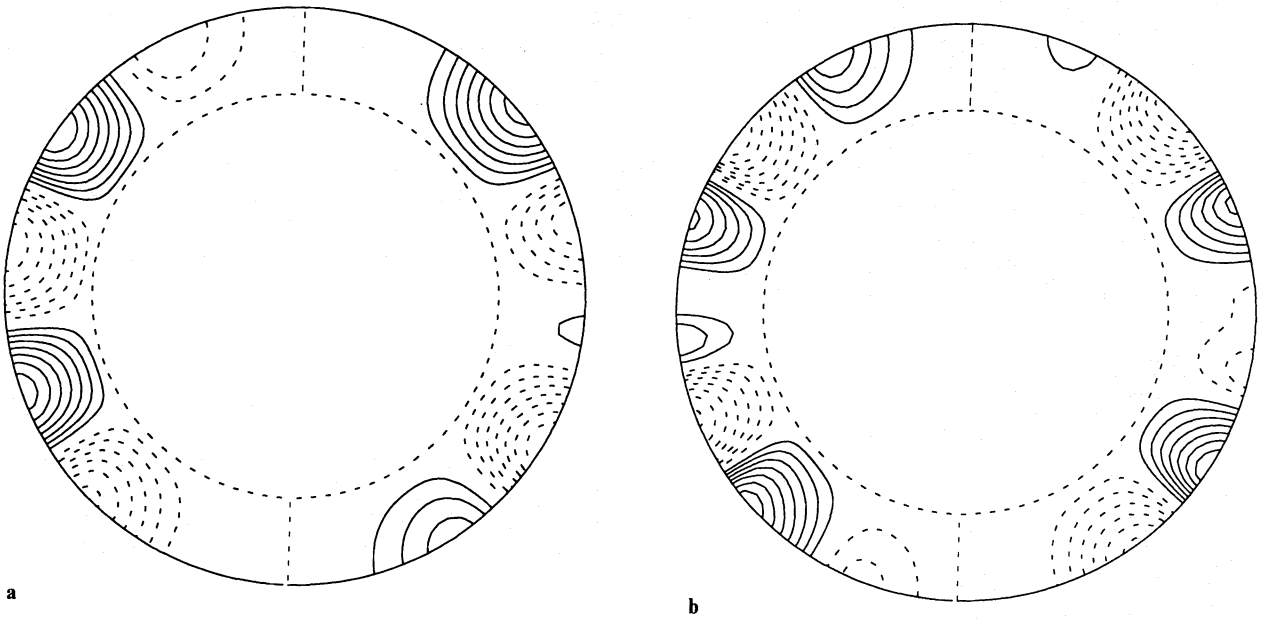

Fig. 4a and b. Field structure, mixed mode, $x_1 = 0.7$. **a** $C_\alpha = 3$, **b** $C_\alpha = 10$

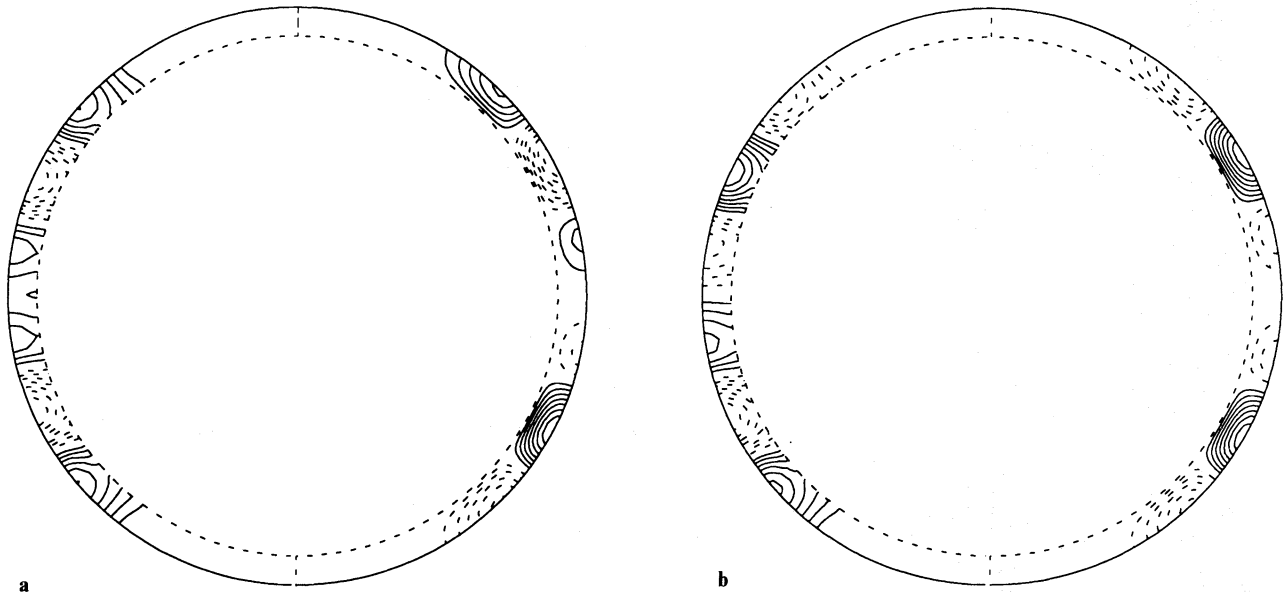

Fig. 5a and b. $x_1 = 0.9$. **a** Eigenmode, $P = -1$, $C_\omega = -10^3$. **b** Eigenmode $P = \pm 1$, $C_\omega = -10^3$

© European Southern Observatory • Provided by the NASA Astrophysics Data System

1990A&A...240..142M

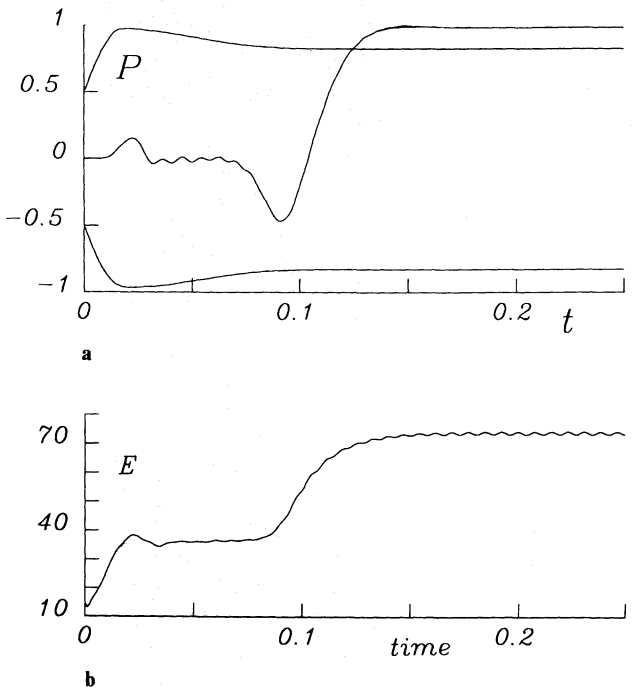

Fig. 6a and b. $x_1 = 0.9$, $C_\omega = -10^3$, $C_\alpha = 10$. **a** Evolution of $P(t)$, $P(0)$ varying, **b** Evolution of E for $P(0) = 0.0$

Table 1. Summary of calculations with $x_1 = 0.7$, $C_\omega = -10^3$ and $P(0) = 0$. $\langle P \rangle$ is the mean value of P. Amplitudes of oscillations are indicated by $\pm$, except in cases marked by an asterisk where the amplitude is very small

C_α	log E	$\langle P \rangle (t \simeq 0.6)$	Period
1.5	0.45 ± 0.10	$\rightarrow -1$?	0.098
2.0	1.07 ± 0.07	0.165 ± 0.01	0.084
3.0	1.57 ± 0.05	0.01 ± 0.01	0.064
5.0	2.03 ± 0.03	-0.19 ± 0.01	0.048
7.0	2.32 ± 0.02	-0.365*	0.040
10.0	2.52 ± 0.02	-0.45*	0.033
20.0	2.96 ± 0.01	-0.43*	0.023

Table 2. Summary of calculations with $x_1 = 0.9$, $C_\omega = -10^3$ and $P(0) = 0$ at time t when behaviour is quasi-steady. $\langle P \rangle$ is the mean value of P. Amplitudes of oscillations are indicated by $\pm$, except in cases marked by an asterisk where the amplitude is very small

C_α	t	log E	$\langle P \rangle (t)$	Period
4	0.6	0.970 ± 0.005	0.69*	0.028
7	0.325	1.531 ± 0.005	-0.25 ± 0.01	0.019
10	0.25	1.869 ± 0.003	0.987	0.0155
20	0.325	2.374 ± 0.003	0.27 ± 0.01	0.011

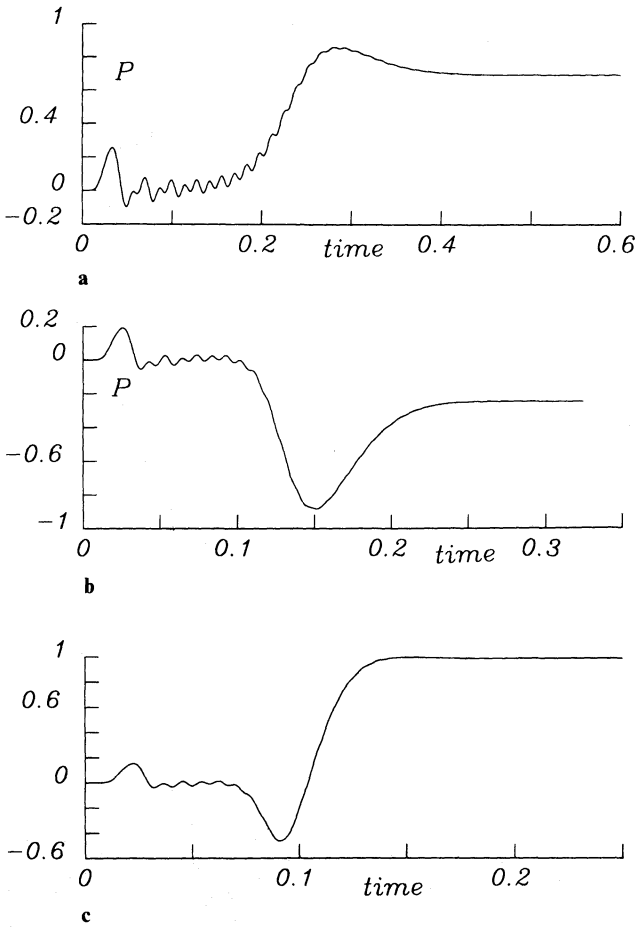

Fig. 7a–c. Evolution of $P(t)$ for calculations with $P(0) = 0.0$, $x_1 = 0.9$, $C_\omega = -10^3$ for **a** $C_\alpha = 4$, **b** $C_\alpha = 7$, **c** $C_\alpha = 10$

4. Discussion

Examination of the pure parity solutions shows that the field structure for A0 and S0 modes is remarkably similar. This phenomena has been observed previously for dynamo models in spherical shells (e.g. Brandenburg et al. 1990), but several other features of these thin shell dynamos are rather different in nature from those for more 'global' models. For example, when the initial field has mixed parity, there is no rapid evolution to one of a few final states – either of pure or mixed parity (the latter being perhaps a limit cycle or torus; see Brandenburg et al. 1989 and Paper I). Instead the solutions settle to a common frequency and energy for given parameters C_α and C_ω, but with very slowly changing oscillations in P. The mean value of P then depends on the initial conditions, in what in some cases appears to be a somewhat non-uniform manner (see, e.g., Figs. 2 and 6). We speculate that this unsystematic behaviour may be caused by the initial field configurations [with various $P(0)$] being quite distant in structure from the almost steady limit cycles found in the phase of slow evolution, and that in the initial phase of rapid relaxation, where perhaps numerical inaccuracies are larger than subsequently, some of the 'memory' of the initial state is lost. Choosing a set of initial states, of varying $P(t=0)$ that are less distant from the final field configurations would probably remove this feature.

© European Southern Observatory • Provided by the NASA Astrophysics Data System

1990A&A...240..142M

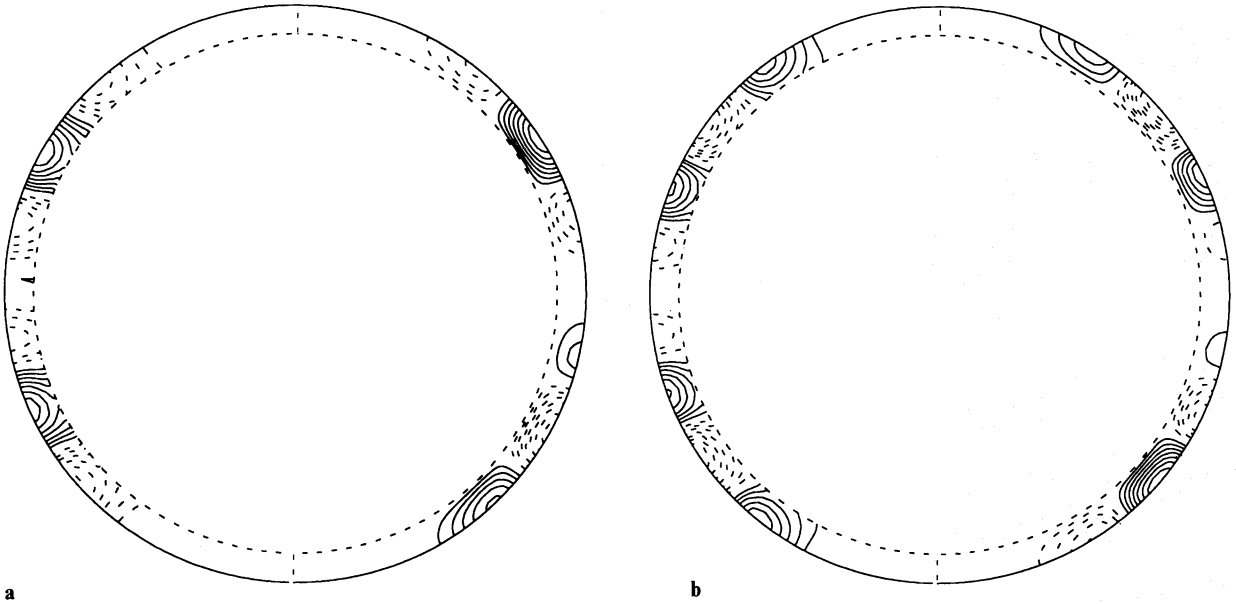

Fig. 8a and b. Field structure, mixed mode, $x_1 = 0.9$, $C_\omega = -10^3$. **a** $C_\alpha = 4$, **b** $C_\alpha = 10$

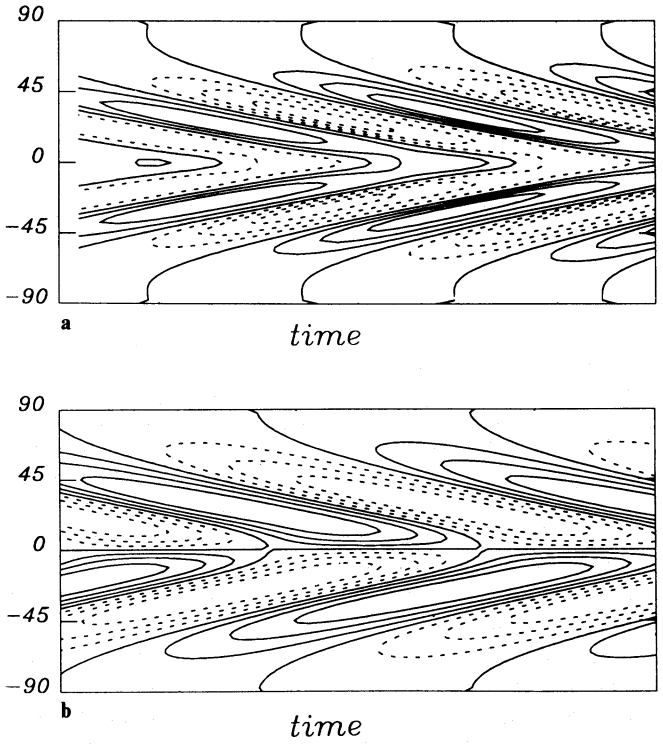

Fig. 9a and b. Butterfly diagrams (toroidal field strength just below $x = 1$), odd parity fields for **a** thin shell, $C_\alpha = 2.5$, **b** thick shell, $C_\alpha = 4.0$. Time runs from left to right, the ordinates are degrees of latitude

The fact that the mean parity of many of our solutions does appear to be changing very slowly after an initial rapid relaxation may indicate an ultimate preference for one of a few stable solutions. However $d\langle P\rangle/dt$ is so small that following the field evolution for a significant length of time is prohibitively expensive in terms of computer time. The *initial* rate of change of parity is less significant, as it is strongly influenced by the choice of initial field configuration. It should be noted that this phenomenon of slowly changing $\langle P\rangle$ is not peculiar to buoyancy quenched models, but has also been observed for α-quenched shell dynamos (cf. Brandenburg et al. 1990).

The apparent lack of a clear preference for any definite pure parity solution may be jointly attributable to the very similar bifurcations and growth rates of the A0 and the S0 modes and to the small aspect ratio of the shell (especially when $x_1 = 0.9$). The latter seems to favour the break up of the field structure into more-or-less isolated cells with little direct interaction with one another. This is probably encouraged, partly at least, by our simple, local boundary condition on a, in contrast to the global condition of fitting to a curl-free external field that is usually employed when modelling dynamos in a complete convective envelope. We note that our boundary condition may have some real relevance to a dynamo situated at the bottom of a convective envelope of a solar type star: the poloidal field is relatively weak and is likely to suffer massive distortion in the turbulent envelope. In addition, at the solar surface the large-scale poloidal field is difficult to observe, but the region immediately external to the photosphere is not curl-free and there is really no reason, apart from mathematical convenience, to adopt the global curl-free condition there. Thus the (perhaps ill-known) connection between the boundary conditions and the detailed field structure at the photosphere and a shell dynamo deep in the interior may in practice be quite tenuous.

Attempts to model thin layer dynamos by removing one or more of the spatial dimensions, typically replacing the corresponding derivatives by order of magnitude estimates, give sets of equations that are more tractable either numerically or analytically. The solution of such systems can, for example, be followed to much larger dynamo numbers than is the case for our model (e.g. Jennings & Weiss 1990). However the result usually found is

© European Southern Observatory • Provided by the NASA Astrophysics Data System

1990A&A...240..142M

that the relevant modes are those with the greatest spatial extent in the latitudinal (i.e. θ-) direction. Our result that the preferred modes often have a cell-like structure clearly throws doubt on the applicability of such truncated, one-dimensional models.

Butterfly diagrams for typical odd parity thick and thin shell models are shown in Fig. 9, remembering, of course, that they refer to the field just below the shell surface and not the stellar surface. They display the usual equatorward migration to be expected from $\alpha\omega$ dynamos with our choice of parameters, although the cell-like structure of the field means there is considerable θ-structure. For the "thin shell" models the number of "belts" in each hemisphere is approximately three (Fig. 9a), compared with a figure of about two for the "thick shell" models (Fig. 9b). This might be compared with the solar value of two. These numbers do depend somewhat on the magnitude of C_α and, again, the link with an "observable" field might be remote. As expected with $\alpha > 0$ in the northern hemisphere, B_r and B_φ are in antiphase (Stix 1976; Yoshimura 1976). However it is probable that α changes sign at the bottom of the convection zone. If also $\Omega_0' > 0$ in this region (e.g. Brown et al. 1989) the "correct" butterfly diagram (equatorward migration) could be recovered, but with B_r and B_φ in phase, in contrast to the observed solar field. It is quite uncertain whether the diffusive layer above a bottom dynamo could alter the phase relation. A large scale laminar circulation in the overlying region could possibly also effect the direction of field migration at the surface. Calculations incorporating both the "bottom dynamo" region and the overlying envelope are necessary to answer this question.

Acknowledgement. This work was done whilst DM was a visitor to the Helsinki Observatory under the Royal Society – Finnish Academy of Sciences Exchange Agreement.

References

Brandenburg A., Krause F., Meinel R., Moss D., Tuominen I., 1989, A&A 213, 411
Brandenburg A., Moss D., Tuominen I., 1989, Geophys. Astrophys. Fluid Dyn. 49, 129
Brandenburg A., Meinel R., Moss D., Tuominen I., 1990, in: Solar photosphere: Structure, Convection and Magnetic Fields, ed. J.O. Stenflo, Kluwer, Dordrecht, p. 379
Brown T.M., Christensen-Dalsgaard, J., Dziembowski W.A., Goode P., Gough D., Morrow C.A., 1989, ApJ 343, 526
DeLuca E.E., Gilman P.A., 1986, Geophys. Astrophys. Fluid Dyn. 37, 85
Jennings R., Weiss N.O., 1990, in: Solar Photosphere: Structure, Convection and Magnetic Fields, ed. J.O. Stenflo, Kluwer, Dordrecht, p. 355
Krivodubskii V.N., 1984, Sov. Astron. 28, 205
Leighton R.B., 1969, ApJ 156, 1
Moss D., Tuominen I., Brandenburg, A., 1990, A&A 228, 284
Noyes R.W., Weiss N.O., Vaughan A., 1984, ApJ 287, 769
Rädler K.-H., 1990, in: Inside the Sun, IAU Colloq. 121, ed. G. Berthomieu, M. Cribier, Kluwer, Dordrecht, p. 385
Schmitt D., Schüssler M., 1989, A&A 223, 343
Stix M., 1976, A&A 47, 243
Yoshimura H., 1976, Solar Phys. 50, 3

© European Southern Observatory • Provided by the NASA Astrophysics Data System